

Small Molecule Binding to the Mixed-Valent Diiron Center of Methane Monooxygenase Hydroxylase from *Methylococcus capsulatus* (Bath) as Revealed by ENDOR Spectroscopy

Jean-Paul Willems,[†] Ann M. Valentine,[‡] Ryszard Gurbiel,[†] Stephen J. Lippard,^{*,‡} and Brian M. Hoffman^{*,†}

Contribution from the Department of Chemistry, Northwestern University, Evanston, Illinois 60208-3113, and Department of Chemistry, Massachusetts Institute of Technology, Cambridge, Massachusetts 02139-4307

Received March 9, 1998

Abstract: The binding of several exogenous molecules at the active site of the soluble methane monooxygenase hydroxylase (MMOH) from *Methylococcus capsulatus* (Bath) is described. The interaction of methanol, the product of methane hydroxylation, with the mixed-valent Fe^{II}Fe^{III} form of the enzyme induces a change in the EPR spectrum of the unmodified protein from $g = 1.940, 1.865, \text{ and } 1.740$ to one with $g_1 = 1.963$ and $g_2 = 1.862$. This spectral change arises from the coordination of methanol to the diiron center, as demonstrated by electron nuclear double resonance (ENDOR) spectroscopic studies of mixed-valent MMOH prepared with CD₃OH added to a DMSO-treated sample, which displayed a ²H interaction with an isotropic hyperfine splitting of ~0.5 MHz. A detailed analysis indicates that methanol binds to the ferrous iron without displacing a terminally bound water molecule identified previously. Acetate labeled with ¹³C at the carboxylate carbon atom also gives rise to ENDOR signals, whereas no such signals are seen when the label is at the methyl carbon atom or when the methyl group is deuterated. These results suggest that acetate is oriented in the active site with its carboxylate group pointing toward the iron center, confirming a previous interpretation of X-ray crystallographic experiments. At the MMOH diiron core, four coordination positions that are not usually occupied by endogenous protein ligands are identified which can simultaneously accommodate DMSO, methanol, and water. The implications of these results for the catalytic mechanism of the enzyme are discussed.

Introduction

An understanding of the intimate mechanism of alkane oxidation by the soluble methane monooxygenase (sMMO) system of proteins^{1–3} requires knowledge of coordination sites at the carboxylate-bridged diiron catalytic center in the hydroxylase enzyme (MMOH) that can be occupied by substrate or product molecules during turnover. X-ray crystal structure studies of MMOH from *Methylococcus capsulatus* (Bath)^{4,5} have revealed four such positions (Figure 1), identified by the fact that they are not usually occupied by protein residues but accommodate ligands contributed by solvent or buffer components.⁶ Electron nuclear double resonance (ENDOR) spectroscopy offers a powerful, selective, and sensitive ally to

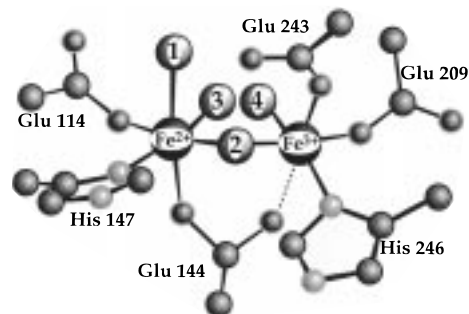


Figure 1. A model of the hydroxylase active site with anchor positions occupied by amino acids and potential catalytic positions numbered 1–4. Fe1 has been modeled as the ferrous iron and Fe2 as the ferric iron^{7,8} (adapted from ref 6).

X-ray crystallography for addressing the question of exogenous ligand binding sites and interrogating metastable intermediates in the reaction cycle. This technique requires a paramagnetic center which, in the case of MMOH, can be obtained by preparing the active site in the mixed-valent Fe^{II}Fe^{III} or Fe^{III}Fe^{IV} states,^{7,9,10} or by analyzing the even-spin diiron-(II)^{11,12} form of the protein.

(8) The opposite assignment was incorrectly given in the ⁵⁷Fe ENDOR results section of ref 7. The remainder of the paper, however, is consistent and describes Fe1 as the ferrous iron and Fe2 as the ferric iron. This assignment is only a working model, and the reverse may be true.

(9) DeRose, V. J.; Liu, K. E.; Kurtz, D. M., Jr.; Hoffman, B. M.; Lippard, S. J. *J. Am. Chem. Soc.* **1993**, *115*, 6440–6441.

* To whom correspondence should be addressed.

[†] Northwestern University.

[‡] Massachusetts Institute of Technology.

(1) Liu, K. E.; Lippard, S. J. *Advances in Inorganic Chemistry*; Academic Press: San Diego, 1995; Vol. 42, p 263–289.

(2) Wallar, B. J.; Lipscomb, J. D. *Chem. Rev.* **1996**, *96*, 2625–2657.

(3) Valentine, A. M.; Lippard, S. J. *J. Chem. Soc., Dalton Trans.* **1997**, *21*, 3925–3931.

(4) Rosenzweig, A. C.; Frederick, C. A.; Lippard, S. J.; Nordlund, P. *Nature* **1993**, *366*, 537–543.

(5) Rosenzweig, A. C.; Nordlund, P.; Takahara, P. M.; Frederick, C. A.; Lippard, S. J. *Chem. Biol.* **1995**, *2*, 409–418.

(6) Whittington, D. A.; Lippard, S. J. In *ACS Symposium Series*; Hodgson, K. O., Solomon, E. I., Eds.; American Chemical Society: Washington, D. C., 1998.

(7) DeRose, V. J.; Liu, K. E.; Lippard, S. J.; Hoffman, B. M. *J. Am. Chem. Soc.* **1996**, *118*, 121–134.

Previously we applied ENDOR spectroscopy to identify a bridging hydroxide at site 2, a terminal DMSO bound to the ferric iron, and protein-derived ligands in mixed-valent sMMO from *M. capsulatus* (Bath).^{7,9,11,12} In the present work, we have extended these studies to provide evidence that the acetate ion binds with its carboxylate group directed toward the diiron center, supporting a previous assignment as the acetate ion of electron density of uncertain origin in X-ray crystal structure maps.^{4,5} We also offer the first direct proof that methanol, the product of methane oxidation by the enzyme, coordinates directly to the diiron center, in contrast to the conclusion of a previous ENDOR study of MMOH from *Methylosinus trichosporium* OB3b.¹³ Finally, we demonstrate that the coordination positions for exogenous ligands denoted in Figure 1 can simultaneously accommodate DMSO, methanol, and water. This information should facilitate both theoretical and experimental investigations of details of the catalytic mechanism of MMOH.

Materials and Methods

Protein Purification. Growth of native *M. capsulatus* (Bath) was carried out as described elsewhere.¹⁴ Purification of MMOH was performed by using a modification of a published procedure.¹⁵ The crude protein obtained from a DEAE Sepharose anion exchange column¹⁶ was pooled and concentrated to approximately 0.2 mM. A 5-mL portion of this crude preparation was loaded onto a Superdex 200 column (2.6 × 80 cm) and eluted with 25 mM MOPS (pH 7.0) containing 120 mM NaCl, 5% glycerol, and 1 mM dithiothreitol. Specific activities and iron content were in the ranges previously described.^{17,18}

Sample Preparation. Solutions of MMOH (1 mM) were prepared by concentrating purified protein with centrifugal concentrators (Centriprep and Centricon, Amicon) having a molecular weight cutoff of 30 000. An electron-transfer mediator solution containing 10 mM phenazine methosulfate, 10 mM methylene blue, and 10 mM potassium indigotetrasulfonate was added to a final concentration of 0.5 mM. The samples were reduced to the Fe^{II}Fe^{III} mixed-valent state, MMOH_{mv}, as reported elsewhere.⁹ In studies with exogenous ligands, the reagents were added prior to reduction; in all of the cases, their final concentration was 0.1 M. Samples in 23% ¹⁷O water were prepared by exchanging the purified hydroxylase into 50 mM MOPS, pH 7.0, twice diluting the sample with an equal volume of H₂¹⁷O, and concentrating it to 1 mM MMOH by using a Microcon centrifugal concentrator (Amicon) with a molecular weight cutoff of 50 000. Isotopically enriched methanol (CD₃OH, 99.5%, or ¹³CH₃OH, 99%), sodium acetate (¹³CH₃CO₂Na, 99%, or CH₃¹³CO₂Na, 99%), and DMSO [(CD₃)₂SO, 99.9%] were obtained from Cambridge Isotope Labs, CD₃-CO₂Na (99%) was purchased from Aldrich, and H₂¹⁷O (30.4%) was supplied by Isotec.

(10) Valentine, A. M.; Tavares, P.; Pereira, A. S.; Davydov, R.; Krebs, C.; Hoffman, B. M.; Edmondson, D. E.; Huynh, B. H.; Lippard, S. J. *J. Am. Chem. Soc.* **1998**, *120*, 2190–2191.

(11) Hoffman, B. M.; Sturgeon, B. E.; Doan, P. E.; DeRose, V. J.; Liu, K. E.; Lippard, S. J. *J. Am. Chem. Soc.* **1994**, *116*, 6023–6024.

(12) Sturgeon, B. E.; Doan, P. E.; Liu, K. E.; Burdi, D.; Tong, W. H.; Nocek, J. M.; Gupta, N.; Stubbe, J.; Kurtz, D. M., Jr.; Lippard, S. J.; Hoffman, B. M. *J. Am. Chem. Soc.* **1997**, *119*, 375–386.

(13) Hendrich, M. P.; Fox, B. G.; Andersson, K. K.; Debrunner, P. G.; Lipscomb, J. D. *J. Biol. Chem.* **1992**, *267*, 261–269.

(14) Pilkington, S. J.; Dalton, H. *Methods In Enzymology*; Academic Press: New York, 1990; Vol. 188; pp 181–190.

(15) Fox, B. G.; Froland, W. A.; Jolliffe, D. R.; Lipscomb, J. D. In *Methods In Enzymology*; Academic Press: New York, 1990; Vol. 188; pp 191–202.

(16) Valentine, A. M.; Wilkinson, B.; Liu, K. E.; Komar-Panicucci, S.; Priestley, N. D.; Williams, P. G.; Morimoto, H.; Floss, H. G.; Lippard, S. J. *J. Am. Chem. Soc.* **1997**, *119*, 1818–1827.

(17) DeWitt, J. G.; Bentsen, J. G.; Rosenzweig, A. C.; Hedman, B.; Green, J.; Pilkington, S.; Papaefthymiou, G. C.; Dalton, H.; Hodgson, K. O.; Lippard, S. J. *J. Am. Chem. Soc.* **1991**, *113*, 9219–9235.

(18) Liu, K. E.; Johnson, C. C.; Newcomb, M.; Lippard, S. J. *J. Am. Chem. Soc.* **1993**, *115*, 939–947.

ENDOR Spectroscopy. The continuous wave (CW) ENDOR spectrometer and the procedures employed in this study have been briefly reported.¹⁹ A description of the 35 GHz pulse ENDOR spectrometer employed in this study has been published recently.²⁰ The proton CW ENDOR spectra were recorded by using “Packet-Shifting” ENDOR.²¹ When studying metalloproteins, using this type of ENDOR spectroscopy has many advantages including excellent signal-to-noise ratios at low sample temperature where relaxation rates are slow. A ¹³C ENDOR signal consists of a doublet centered at the ¹³C Larmor frequency (ν_C) and split by the nuclear hyperfine coupling (A_C); a ²H signal consists of a doublet centered at ν_D and split by A_D , with an additional splitting caused by the nuclear quadrupole interaction.

²H and ¹³C ENDOR spectra were collected by using the Mims stimulated-echo ENDOR pulse sequence.^{22,23} In this protocol, the ENDOR response R depends jointly on the nuclear hyperfine coupling A and the interval between the first and second microwave pulses according to eq 1. This equation shows that the ENDOR response

$$R \propto [1 - \cos(2\pi A\tau)] \quad (1)$$

will fall to zero for integer values of $A\tau$ and will reach a maximum for half-integer $A\tau$ values. Such “hyperfine selectivity” is normally considered to be one of the key benefits of pulsed ENDOR techniques. Orientation-selective ENDOR analysis of frozen solutions relies on accurate line shapes and intensities, however. Our experience with Mims ENDOR of powder or frozen-solution samples shows that one obtains ENDOR patterns essentially undistorted by the blind spots only for couplings in the range $A < 1/(2\tau)$.²⁴ Thus, in practice, in the study of frozen solutions, the maximum hyperfine value, A_{\max} , that should be studied by a Mims ENDOR sequence is restricted by the minimum usable value of τ , denoted as the deadtime, t_d , with the result that $A_{\max} \approx 1/(2t_d)$. The deadtime is defined as the minimum time after the last pulse that the ENDOR effect can be detected against the resonator ringdown, and it depends not only on the spectrometer performance but also on the strength of the ENDOR signal. The value, $\tau = 480$ ns, used in all reported spectra maximizes the sensitivity for a hyperfine value of 1.05 MHz.

Results

EPR Spectroscopy. Both native and dimethyl sulfoxide (DMSO)-treated MMOH_{mv} display an anisotropic g tensor which normally would produce excellent orientation selection at 35 GHz (Figure 2). Native MMOH_{mv}, $g = 1.94(0), 1.86(5), 1.74(0)$, shows a distribution in the values of g_2 and g_3 ,^{25–27} however, which hinders the analysis of the ENDOR data. The EPR spectrum of the DMSO-treated mixed-valent hydroxylase,¹³ MMOH_{mv}[DMSO], $g = 1.95(0), 1.87(0), 1.80(5)$, does not show this distribution in g values, and as a result, gives better orientation-selective ENDOR spectra.⁹ As first reported by others,¹³ addition of methanol to native MMOH_{mv} (Figure 2a) induces clear changes in the EPR spectrum, shifting g_1 to higher (1.963) and g_2 to lower (1.862) values. The addition of methanol to the DMSO treated sample does not further alter the EPR spectrum of MMOH_{mv}[DMSO] (Figure 2b).

ENDOR Spectroscopy. Figure 3 shows 35 GHz Mims pulsed ENDOR spectra of MMOH_{mv} samples treated with

(19) Werst, M. M.; Davoust, C. E.; Hoffman, B. M. *J. Am. Chem. Soc.* **1991**, *113*, 1533–1538.

(20) Davoust, C. E.; Doan, P. E.; Hoffman, B. M. *J. Magn. Reson., Ser. A* **1996**, *119*, 38–44.

(21) DeRose, V. J.; Hoffman, B. M. *Methods In Enzymology*; Academic Press: New York, 1995; Vol. 246, p 554–589.

(22) Mims, W. B. *Proc. R. Soc. London* **1965**, *283*, 452–457.

(23) Gemperle, C.; Schweiger, A. *Chem. Rev.* **1991**, *91*, 1481–1505.

(24) Doan, P. E.; Fan, C.; Hoffman, B. M. *J. Am. Chem. Soc.* **1994**, *116*, 1033–1041.

(25) Froncisz, W.; Hyde, J. S. *J. Chem. Phys.* **1980**, *73*, 3123–3131.

(26) Hagen, W. R. *J. Magn. Reson.* **1981**, *44*, 447–469.

(27) Hagen, W. R. In *Advanced EPR: Applications in Biology and Biochemistry*; Hoff, A. J., Ed.; Elsevier: Amsterdam, 1989.

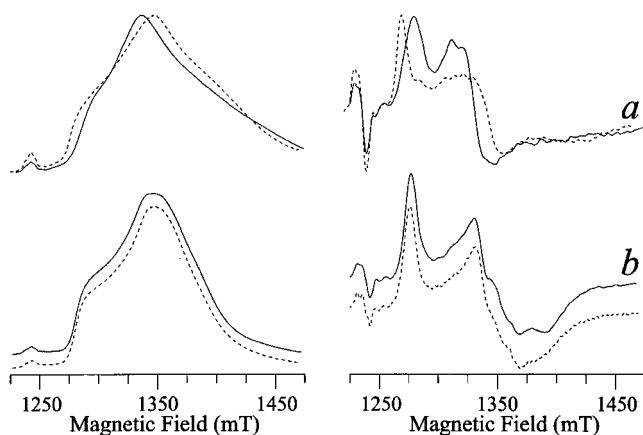


Figure 2. Series of 35 GHz CW EPR spectra of MMOH_{mv} . Left, EPR absorption envelopes obtained from 100 kHz detection under conditions of rapid passage; right, numerical derivatives of these spectra. (a) Solid line: native MMOH_{mv} , microwave frequency 34.955 GHz, modulation amplitude 2.5 G. Dashed line: methanol added to the native protein, microwave frequency 34.988 GHz, modulation amplitude 2 G. (b) Solid line: MMOH_{mv} treated with DMSO, microwave frequency 35.008 GHz, modulation amplitude 2 G. Dashed line: methanol added to the previous sample, microwave frequency 35.013 GHz, modulation amplitude 2 G.

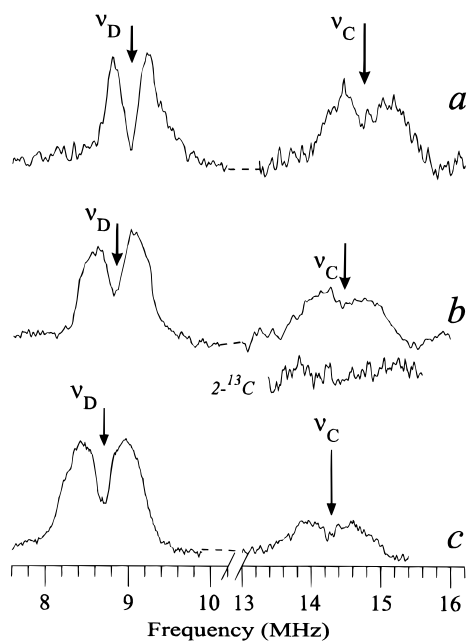


Figure 3. Series of 35 GHz pulsed Mims ENDOR spectra of MMOH_{mv} at a field position corresponding to g_3 . The ^2H and ^{13}C Larmor frequencies are indicated by black arrows. (a) MMOH_{mv} with deuterated methanol in the presence of $1\text{-}^{13}\text{C}$ -acetate, microwave frequency 34.741 GHz, $\tau = 480$ ns. The field position corresponds to g_3 . (b) $\text{MMOH}_{\text{mv}}\text{-[DMSO}(d_6)]$ with $1\text{-}^{13}\text{C}$ -acetate, microwave frequency 34.657 GHz, $\tau = 480$ ns. The field corresponds to a value between g_2 and g_3 . A spectrum of a sample prepared with $2\text{-}^{13}\text{C}$ -acetate was recorded in the ^{13}C frequency range (13–15.5 MHz) and is depicted under that of the labeled sample. (c) ^{13}C -labeled methanol added to $\text{MMOH}_{\text{mv}}\text{[DMSO}(d_6)]$, microwave frequency 34.734 GHz, $\tau = 480$ ns. This spectrum is recorded at a g_2 . In all of the spectra, the rf pulse width was 60 μs , the microwave pulse width was 48 ns, and $T = 2$ K.

various reagents. Each spectrum is taken at the magnetic field which gives the best signal-to-noise ratio for the specific sample. These spectra are composites of subspectra taken in the vicinity of the ^2H Larmor frequency as well as the ^{13}C Larmor frequency, which are denoted by arrows.

Addition of Methanol and Acetate to MMOH_{mv} . Figure 3a presents a ^2H Mims ENDOR spectrum of native MMOH_{mv} to which deuterated methanol and $[^{13}\text{C}_1]$ -acetate, hereafter $1\text{-}^{13}\text{C}$ -acetate, have been added. The ENDOR spectrum clearly shows a resolved ^2H signal comprising a pair of featureless peaks split by the hyperfine coupling, $A(^2\text{H}) \approx 0.5$ MHz; the quadrupole splitting is smaller than the line width of the peaks and is therefore indistinguishable. This ^2H signal is the same as that in the absence of acetate. The small change in the EPR spectrum seen upon methanol addition is therefore not a consequence of nonspecific, solvent-induced protein perturbations; the observation of this ENDOR signal establishes that methanol is incorporated into the active site of the enzyme. The existence of substantial hyperfine splitting, which corresponds to $A(^1\text{H}) \approx 3.3$ MHz, strongly suggests that methanol binds directly to iron. The small change in the EPR spectra further indicates that this binding is not accompanied by a major structural perturbation, although a carboxylate shift or displacement of the water/hydroxide ligand coordinated to Fe^{II} as identified by ENDOR spectroscopy may have occurred.⁷

The sample includes $1\text{-}^{13}\text{C}$ -acetate in the solution, and its ENDOR spectra show a low-intensity ^{13}C peak centered at the ^{13}C Larmor frequency (Figure 3a). This peak is present in mixed-valent enzyme prepared with $1\text{-}^{13}\text{C}$ -acetate both without (data not shown) and with methanol present, indicating that acetate can be accommodated at the diiron center in a site where it is not displaced by methanol. A ^{13}C signal could not be detected when $2\text{-}^{13}\text{C}$ -acetate was employed (Figure 3b), nor could a ^2H signal be seen when deuterated acetate was used (data not shown). These observations indicate that the acetate is positioned with its carboxyl group pointing toward the diiron center.

Addition of DMSO and Acetate to MMOH_{mv} . Figure 3b presents an ENDOR spectrum of MMOH_{mv} with ^2H -DMSO prepared in the presence of ^{13}C -labeled acetate. This spectrum shows a ^2H signal from the ^2H -DMSO and a ^{13}C ENDOR signal from acetate. Thus, binding of DMSO to the Fe^{III} ion⁷ does not preclude incorporation of acetate into the active site. An attempt was made to obtain a full 2-D data set of ENDOR spectra in order to determine the $1\text{-}^{13}\text{C}$ hyperfine tensor of labeled acetate incorporated into $\text{MMOH}_{\text{mv}}\text{[DMSO]}$. The presence or absence of an isotropic ^{13}C hyperfine component would show whether acetate actually is coordinated to the diiron center. Unfortunately, at g values higher than g_2 the intensity of the ^{13}C ENDOR signals dropped below a detectable level, and the ENDOR pattern of ^{13}C -labeled acetate could be recorded only for g values between g_2 and g_3 . Although the shape of the ^{13}C ENDOR signal in Figure 3b is slightly different from that in Figure 3a, the differences are too small and the signal-to-noise ratio of the ^{13}C spectra is too low to allow any meaningful interpretation.

DMSO and Methanol Binding to MMOH_{mv} . DMSO binds to the Fe^{III} site of the valence-localized mixed-valent diiron center, changing its EPR signal (Figure 2) and giving rise to ^2H ENDOR and ESEEM spectra when deuterated DMSO is utilized.⁷ A spectrum of $\text{MMOH}_{\text{mv}}\text{[}^2\text{H-DMSO]}$ prepared with ^{13}C -methanol shows both a ^2H signal from ^2H -DMSO, as well as a ^{13}C ENDOR signal from the labeled methanol (Figure 3c). Thus, the diiron site can *simultaneously* accommodate DMSO and methanol, which do not compete for the same coordination position. The changes in the EPR signal upon treatment of native MMOH_{mv} with DMSO and methanol separately show that each by itself binds to the iron cluster with complete site

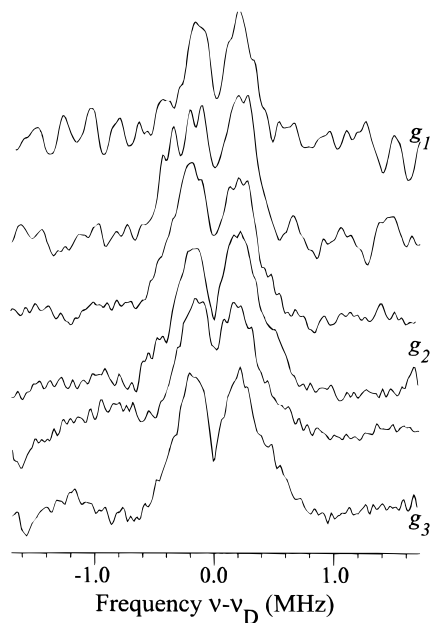


Figure 4. Series of 35 GHz Mims ENDOR spectra across the EPR envelope of $\text{MMOH}_{\text{mv}}[\text{DMSO}]$ with deuterated methanol, rf pulse width 60 μs , microwave pulse width 40 ns, $\tau = 480$ ns, microwave frequency 34.68 GHz, temperature 2 K. The spectra are centered around the ^2H Larmor frequency.

occupancy. The fact that the ^2H spectra from ^2H -DMSO (Figures 3b and 3c) and ^2H -MeOH (Figure 3a) have a better signal-to-noise ratio than the ^{13}C spectrum of ^{13}C -MeOH (Figure 3b) shows that the intensities of the ^{13}C signals in different protein states cannot be used reliably to deduce site occupancies.

Although the addition of methanol to $\text{MMOH}_{\text{mv}}[\text{DMSO}]$ causes no appreciable changes in its EPR spectrum, when deuterated methanol is used, one obtains ^2H ENDOR spectra (Figure 4). With the aim of determining the details of methanol binding, we collected a full 2-D field-dependent ^2H ENDOR pattern from $\text{MMOH}_{\text{mv}}[\text{DMSO}]$ prepared in the presence of ^2H -methanol (Figure 4). The observed ENDOR signals are a statistical average over the contributions of three ^2H atoms having different orientations with respect to the diiron site and, hence, different dipolar hyperfine tensors. As a result, it was not possible to determine precisely the individual ^2H hyperfine tensors. Numerous simulations of the 2-D data, in which we assumed hyperfine tensors that ranged from purely dipolar to nearly isotropic, indicated that the experimental pattern does not exhibit the strong dependence on the field expected for a purely dipole-coupled nucleus and that the ^2H couplings have a substantial isotropic component, $A_{\text{iso}}(^2\text{H}) \approx 0.5$ MHz. This result implies that the methanol molecule is coordinated to the diiron cluster rather than merely being held nearby. The simulations further suggest that the largest component of the dipolar contribution can be no greater than $T(^2\text{H})_{\text{max}} \approx 0.4$ MHz ($T(^1\text{H})_{\text{max}} \approx 2.6$ MHz). Calculations of the dipolar interaction for a proton on a ligand bound to a diiron center^{28,29} indicate that this value is too small for methanol to be bound to Fe^{III} or to be an alkoxo bridge. We therefore conclude that the methanol molecule is bound to the Fe^{II} . The intensity of the ^{13}C ENDOR signals is too low to allow a reliable analysis of the ^{13}C hyperfine tensor as corroboration.

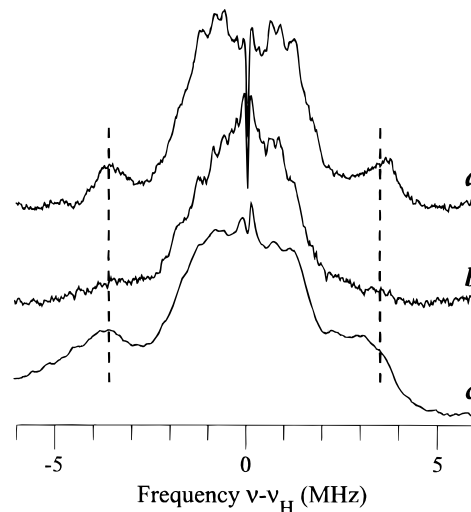


Figure 5. Series of 35 GHz CW ^1H ENDOR spectra of MMOH_{mv} at g_1 . All of the spectra have been centered around the ^1H Larmor frequency. (a) MMOH_{mv} in H_2O , microwave frequency 35.1 GHz, modulation amplitude 0.17 G, modulation frequency 100 kHz, rf scan speed 0.5 MHz/s. rf frequency sweep from low frequency to high. (b) MMOH_{mv} in D_2O as in (a). (c) MMOH_{mv} treated with deuterated methanol in H_2O , microwave frequency 34.9 GHz, modulation amplitude 4 G, modulation frequency 100 kHz, rf scan speed 1 MHz/s. rf frequency sweep from low frequency to high.

Our earlier work⁷ revealed that there is an aqua ligand attached to the Fe^{II} ion of $\text{MMOH}_{\text{mv}}[\text{DMSO}]$. This study further indicated that each iron atom has six ligands bound to it. If methanol binds to the diiron site of $\text{MMOH}_{\text{mv}}[\text{DMSO}]$, either a carboxylate group must shift to accommodate the incoming ligand, or the water molecule bound to Fe^{II} must be displaced by methanol. As a first attempt to evaluate these possibilities, CW ^1H ENDOR spectra were recorded to see whether the exchangeable proton signals assigned to the aqua ligand disappear when methanol binds. In accord with previous observations,⁷ MMOH_{mv} shows ^1H ENDOR signals with $A \approx 7$ MHz (Figure 5a) that arise from an exchangeable aqua ligand. The signals disappear when MMOH_{mv} is exchanged in D_2O buffer (Figure 5b). ^2H -MeOH was added to MMOH_{mv} , with the deuteration acting to suppress any possible proton signals from bound methanol. The resulting ^1H ENDOR spectrum (Figure 5c) also shows a signal from exchangeable proton(s) with $A \approx 7$ MHz but with slightly different line shapes. Similar results are found for $\text{MMOH}_{\text{mv}}[\text{DMSO}]$. These CW ^1H ENDOR data indicate either that water/hydroxide and methanol are simultaneously bound to Fe^{II} or that a methanol replaces the aqua ligand and the OH-proton of methanol gives comparable ^1H CW ENDOR spectra.

To distinguish between these two possibilities, we performed ^{17}O ENDOR studies on $\text{MMOH}_{\text{mv}}[\text{DMSO}]$ in H_2^{17}O buffer, both in the presence and absence of methanol. Figure 6 shows three CW ENDOR spectra taken at a field position corresponding to g_1 . The dotted spectrum represents the ENDOR signal of a sample which had not been labeled with ^{17}O and can therefore be used as a reference. This reference spectrum displays sharp intense peaks at 8.7 and 12.2 MHz as well as some less intense, broader signals at 10 and 14 MHz. The signal at 8.7 MHz is located at the Larmor frequency of ^2H and can be attributed to the ^2H nuclei of labeled methanol. All other signals can be assigned to the ν_+ transitions of ^{14}N . The spectrum displayed using a dashed line shows the ENDOR signal of $\text{MMOH}_{\text{mv}}[^2\text{H}\text{-DMSO}]$ in H_2^{17}O buffer. The presence of an additional, rather broad, featureless ^{17}O signal with a maximum intensity

(28) Willems, J.-P.; Lee, H.-I.; Burdi, D.; Doan, P. E.; Stubbe, J.; Hoffman, B. M. *J. Am. Chem. Soc.* **1997**, 98166–9824.

(29) Randall, D. W.; Gelasco, A.; Caudle, M. T.; Pecoraro, V. L.; Britt, R. D. *J. Am. Chem. Soc.* **1997**, 119, 4481–4491.

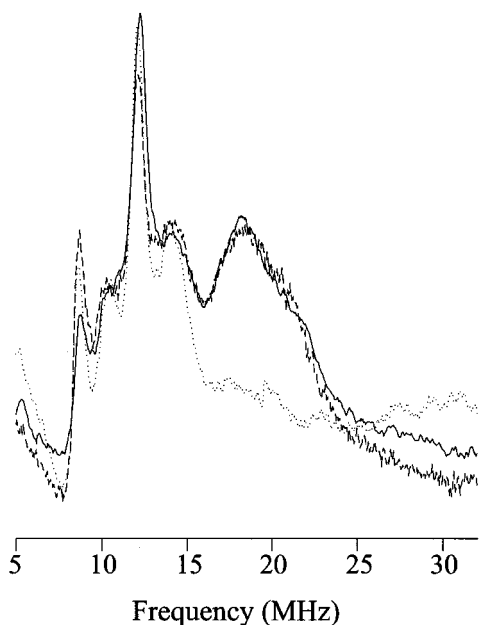


Figure 6. Series of 35 GHz CW ENDOR spectra of MMOH_{mv} at g_1 . Dotted line: $\text{MMOH}_{\text{mv}}[\text{DMSO}]$ with deuterated methanol, microwave frequency 34.991 GHz. Dashed line: $\text{MMOH}_{\text{mv}}[{}^2\text{H-DMSO}]$ exchanged in H_2^{17}O , microwave frequency 35.054 GHz. Solid line: $\text{MMOH}_{\text{mv}}\text{-}[\text{DMSO}]$ with deuterated methanol and exchanged in H_2^{17}O , microwave frequency 35.119 GHz. In all of the spectra, the modulation amplitude was 8 G, modulation frequency 100 kHz, rf scan speed 1 MHz/s, rf frequency sweep from low frequency to high, and temperature 2 K.

at 18.2 MHz is obvious. The ENDOR spectrum of $\text{MMOH}_{\text{mv}}\text{-}[\text{DMSO}]$ in H_2^{17}O buffer in the presence of deuterated methanol (solid line) is almost identical to that of $\text{MMOH}_{\text{mv}}[\text{DMSO}]$ in H_2^{17}O buffer without methanol. It shows the ${}^2\text{H}$ signal of methanol as well as the oxygen signal of water. The simplest interpretation of this result is that the observed ${}^{17}\text{O}$ ENDOR signal from $\text{MMOH}_{\text{mv}}[\text{DMSO}]$ in H_2^{17}O buffer arises from the labeled aqua ligand and that it is not displaced by methanol. An alternative interpretation might be that ${}^{17}\text{O}$ exchanges into the bridge as well as into the terminal aqua site and that methanol displaces only the ${}^{17}\text{O}$ aqua ligand. In such a model, the ${}^{17}\text{O}$ signal from $\text{MMOH}_{\text{mv}}[\text{DMSO}]$ in H_2^{17}O buffer would display both signals, whereas added methanol, by replacing the aqua ligand, would leave an ${}^{17}\text{O}$ signal from the bridge. We do not favor this alternative because we would expect some change in the ${}^{17}\text{O}$ contribution to the spectrum upon the addition of methanol. If a full ${}^{17}\text{O}$ ENDOR pattern across the EPR envelope could be acquired and analyzed, we might be able to confirm the assignment of the oxygen ENDOR signal. Such a determination is not possible because the ${}^{17}\text{O}$ signal broadens and decreases in intensity at higher magnetic field values until it is no longer visible at a field value corresponding to g_2 .

The ENDOR pattern arising from a diiron center containing both a bridging oxygen atom and an oxygen atom terminally attached to Fe^{III} has been well characterized for an $\text{Fe}^{\text{III}}\text{Fe}^{\text{IV}}$ cluster.³⁰ For both oxygen atoms, the hyperfine tensor is almost axial although the A_1 component of the bridging oxygen atom is much smaller than the other two tensor components, whereas the A_1 component of the terminally bound oxygen atom is

significantly larger than A_2 and A_3 . In the case of MMOH_{mv} , we are not able to determine the full hyperfine tensor for ${}^{17}\text{O}$, but the ${}^{17}\text{O}$ ENDOR pattern shows that A_1 is larger than both A_2 and A_3 . This observation supports our conclusion that the oxygen atom from water binds terminally to the Fe^{II} ion in MMOH_{mv} .

Discussion

The observation of ENDOR signals from acetate shows this ion to be located in the vicinity of the diiron cluster of MMOH_{mv} , confirming the assignment of electron density in the X-ray structure as acetate and its orientation with respect to the iron atoms.^{4,5} Given the impossibility of collecting a full field dependence of the ${}^{13}\text{C}$ ENDOR data from labeled acetate, it is not possible to prove the presence of isotropic coupling and, hence, that acetate acts as an iron ligand. Combined with the electron density in the crystal structure determination, however, the data confirm our confidence in such an assignment.

Figure 1 shows four positions at the active site of MMOH which can be occupied by exogenous ligands and thus are available for methanol binding. Our previous ENDOR study⁷ revealed that position 2 contains a solvent exchangeable hydroxo ion; DMSO was modeled at position 4. The study also revealed that a water molecule resides either at site 1 or 3. In the current work, and within the context of the previous model, the remaining site, either 3 or 1, can be occupied by coordinated methanol. Simulations of the ENDOR data suggest that methanol is bound to Fe^{II} . These conclusions further support the idea that acetate does not bind to the diiron center when a sufficient number of exogenous molecules is present to occupy all the available sites (A.M.V., unpublished results). The relative inability of acetate to compete for binding sites is supported by its inability to inhibit catalytic activity. That acetate can be contained in the active site but not ligated to iron is in agreement with previous X-ray crystallographic studies. This work indicated that the bidentate bridging ligand assigned as acetate in the structure of MMOH_{ox} at 4 °C is replaced by a monatomic water bridge in the structure determined at -160 °C.⁵

Combining the results of the current investigation with those of previous X-ray⁵ and ENDOR⁷ studies, we can speculate on aspects of the MMOH mechanism of methane oxidation (Figure 7), while recognizing as important caveats that the diiron center has an oxidation level in the ENDOR experiment not yet observed in the catalytic cycle and that the coupling protein MMOB is not present. The structure of the reduced, diferrous MMOH (H_{red}) in the absence of MMOB is known from X-ray crystallography. It has a bridging carboxylate ligand, Glu243, which is carboxylate-shifted relative to the resting oxidized configuration. The first isolable intermediate in the reaction of dioxygen with diferrous MMOH is a putative peroxodiiron(III) species designated H_{peroxo} . Previously we suggested that O_2 coordinates at the site where DMSO binds to the cluster, site 4 in Figure 1.⁷ In Figure 7, we depict the peroxo moiety bound in sites (3,4) and 2. This formulation agrees with the previous suggestion, as well as with spectroscopic data,³¹⁻³³ theoretical calculations,^{34,35} and results from model compounds,³⁶⁻³⁸ but it is not a unique interpretation. The H_{peroxo} intermediate converts to a high-valent species designated Q which has been characterized by a variety of techniques.^{10,31,33,39-41}

(30) Burdi, D.; Sturgeon, B. E.; Tong, W. H.; Stubbe, J.; Hoffman, B. M. *J. Am. Chem. Soc.* **1996**, *118*, 281-282.

(31) Liu, K. E.; Wang, D.; Huynh, B. H.; Edmondson, D. E.; Salifoglou, A.; Lippard, S. J. *J. Am. Chem. Soc.* **1994**, *116*, 7465-7466.

(32) Liu, K. E.; Valentine, A. M.; Qiu, D.; Edmondson, D. E.; Appelman, E. H.; Spiro, T. G.; Lippard, S. J. *J. Am. Chem. Soc.* **1995**, *117*, 4997; **1997**, *119*, 11134.

(33) Liu, K. E.; Valentine, A. M.; Wang, D.; Huynh, B. H.; Edmondson, D. E.; Salifoglou, A.; Lippard, S. J. *J. Am. Chem. Soc.* **1995**, *117*, 10174-10185.

(34) Siegbahn, P. E. M.; Crabtree, R. H. *J. Am. Chem. Soc.* **1997**, *119*, 3103-3113.

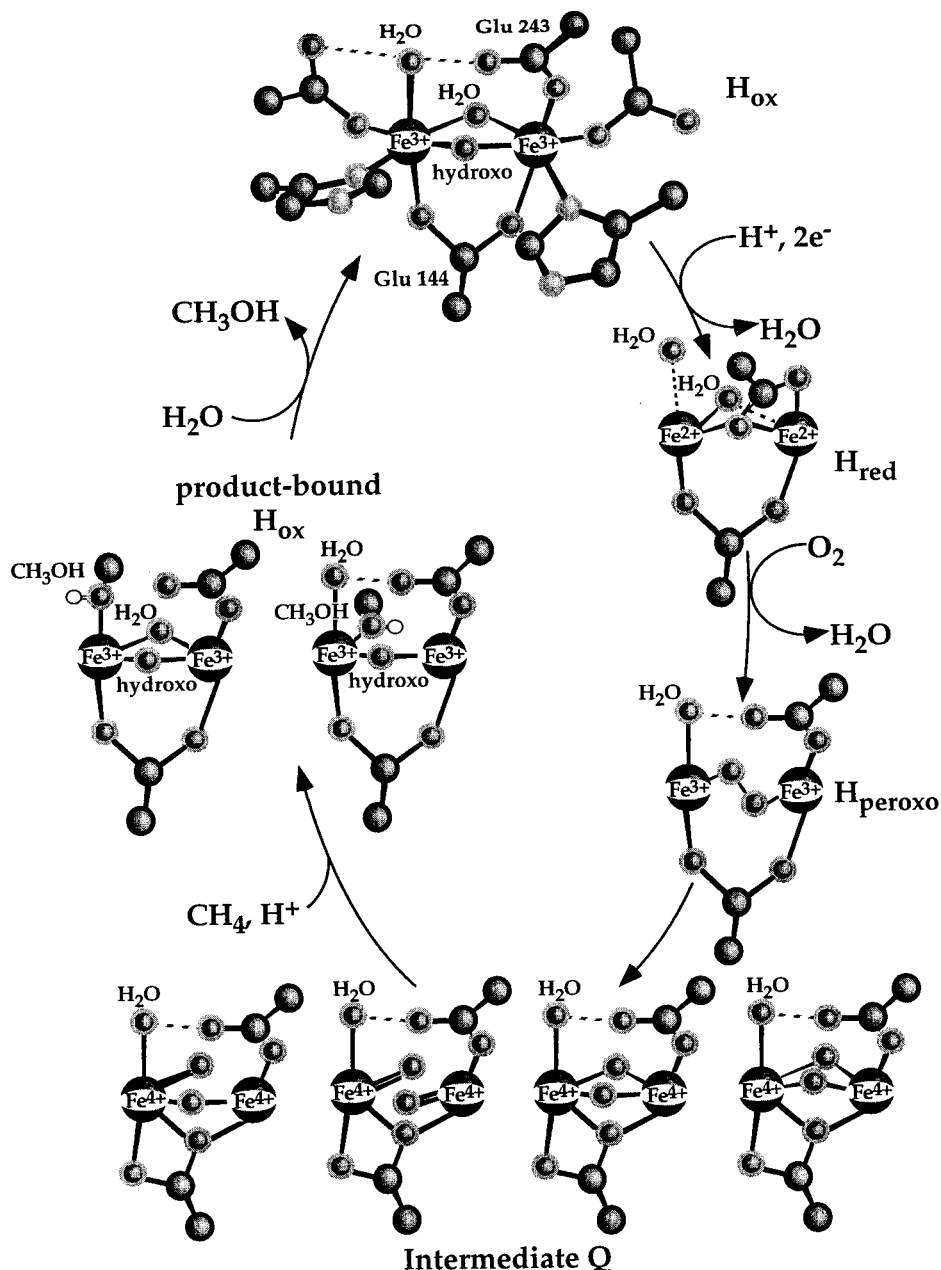


Figure 7. Catalytic cycle of sMMO, depicting the likely binding sites for small molecule substrates. Amino acid ligands in anchor positions are omitted in all but the oxidized structure. Glu144 is drawn in a carboxylate-shifted conformation in the structures of intermediate Q to furnish a third single-atom bridge and promote a short $Fe \cdots Fe$ distance. Such a bridge might alternatively be made by a similarly shifted Glu243 or by a solvent-derived oxo moiety. A quadruply bridged structure with Glu144, Glu243, and two oxoligands joining the two Fe atoms would also suffice.

The reaction of Q with methane, whether or not direct interaction of carbon with an iron atom occurs, could, in principle, involve any of the sites 1–4 depicted in Figure 7, at least one of which will contain an oxo ligand derived from the peroxo intermediate. The current ENDOR experiments suggest that the product

methanol binds preferentially to the iron atom which houses the potential binding sites 1 and 3. It is not known whether methanol binds as the neutral molecule⁴² or as methoxide, but it is presumably replaced by a water ligand, following protonation if necessary, to regenerate the resting state of MMOH and complete the catalytic cycle.

(35) Yoshizawa, K.; Yamabe, T.; Hoffmann, R. *New J. Chem.* **1997**, *21*, 151–161.

(36) Kim, K.; Lippard, S. J. *J. Am. Chem. Soc.* **1996**, *118*, 4914–4915.

(37) Dong, Y.; S., Y.; Young, V. G., Jr.; Que, L., Jr. *Angew. Chem., Int. Ed. Engl.* **1996**, *35*, 618–620.

(38) Ookubu, T.; Sugimoto, H.; Nagayama, T.; Masuda, H.; Sato, T.; Tanaka, K.; Madea, Y.; Okawa, H.; Hayashi, Y.; Uehara, A.; Suzuki, M. *J. Am. Chem. Soc.* **1996**, *118*, 701–702.

(39) Lee, S.-K.; Fox, B. G.; Froland, W. A.; Lipscomb, J. D.; Münck, E. *J. Am. Chem. Soc.* **1993**, *115*, 6450–6451.

(40) Lee, S.-K.; Nesheim, J. C.; Lipscomb, J. D. *J. Biol. Chem.* **1993**, *268*, 21569–21577.

(41) Shu, L. J.; Nesheim, J. C.; Kauffmann, K.; Münck, E.; Lipscomb, J. D.; Que, L., Jr. *Science* **1997**, *275*, 515–518.

Conclusion

The current study supplies the first direct proof that methanol binds to the active site of MMOH, inducing a change in the EPR spectrum of the mixed-valent enzyme and giving rise to an ENDOR interaction when labeled methanol is used. Methanol most likely binds to the ferrous iron in $MMOH_{mv}$, modeled

(42) Watton, S. P.; Masschelein, A.; Rebek, J., Jr.; Lippard, S. J. *J. Am. Chem. Soc.* **1994**, *116*, 5196–5205.

as Fe1, and it apparently does so without displacing a bound water molecule. This investigation also confirms the assignment and disposition of the acetate molecule modeled in X-ray crystallographic studies. ENDOR experiments indicate that the active site can accommodate several small molecules bound simultaneously. Comparing the binding of methanol and acetate in the presence and absence of DMSO, the binding site of which in MMOH_{mv}, has been previously identified in MMOH_{mv}, with

the available sites on the iron atoms affords insights into elements of the mechanism of methane oxidation by MMOH.

Acknowledgment. This work was supported by grants from the National Institutes of Health (GM32134 to S.J.L. and HL13531 to B.M.H.).

JA980795Y